Monthly Notices of the ROYAL ASTRONOMICAL SOCIETY

MNRAS **501,** 5042–5050 (2021) doi:10.1093/mnras/staa2261

Fast synthetic spectral fitting for large stellar samples: a critical test with 25 bright stars of known rotation

K.-P. Schröder,[1,2]★ M. Mittag,[3] L. M. Flor Torres,[1] D. Jack [1] and I. Snellen[2]

[1]*Departamento de Astronomía, Universidad de Guanajuato, AP 144, Guanajuato, GTO, CP 36000, Mexico*
[2]*Sterrewacht Leiden, Nils Bohrweg 2, NL-2333CA Leiden, the Netherlands*
[3]*Hamburger Sternwarte, Universität Hamburg, Gojenbergsweg 112, D-21029 Hamburg, Germany*

Accepted 2020 July 24. Received 2020 July 24; in original form 2020 March 5

ABSTRACT

This work presents and tests a reliable, but nonetheless fast, method for determining the physical parameters of large stellar samples with moderate-resolution spectra, with extensive host star–exoplanet studies in mind. The proposed strategy complements spectral synthesis for obtaining spectroscopically sensitive parameters (i.e. effective temperature and rotation velocity) through other data to keep less critical quantities fixed. We test this approach on a sample of 25 bright (4–7 mag), cool main-sequence stars, for which rotation periods are known from chromospheric activity monitoring. On the basis of good-quality (signal-to-noise ratio 70–80) Tracking and Imaging Gamma-Ray Experiment–Heidelberg Extended Range Optical Spectrograph (TIGRE–HEROS) spectra with a modest spectral resolving power of $R = 21\,000$, we employ the fast ISPEC tool. With gravities calculated and approximate metallicities taken from *uvby* photometry (Geneva–Copenhagen catalogue), spectral synthesis is focused on refining the crucial effective temperature. Finally, rotational velocities are fitted. However, these suffer from cross-talk with gravity and convective turbulence. We find that prescribing macroscopic turbulent velocities for most stars within 2–3 km s^{-1} (with 4–6 km s^{-1} for only our three warmest stars) and microscopic turbulent velocities within 0.7–1.5 km s^{-1} (turbulence increasing with effective temperature, from under 5000 K to 6300 K) results in a satisfactory match (with residuals of 2.5 km s^{-1}) of the period-related, very small rotation velocities of our sample stars. With this prescription, the fast spectral synthesis method described yields effective temperatures similar to intensive atmospheric modelling of high-resolution spectra.

Key words: techniques: spectroscopic – stars: activity – stars: chromospheres.

1 INTRODUCTION

With exoplanet research drawing from an ever growing large database, already with about 4000 confirmed cases (see NASA Exoplanet Archive at the IPAC/CalTech), and looming questions about host star–planet relationships and planet formation, it has become ever more important to find an analysis method to determine stellar parameters that is both fast and accurate. It should provide a homogeneous quality of results over very large stellar samples. These are now being extended to cover bright stars in the whole sky by the space missions *Transiting Exoplanet Survey Satellite* (*TESS*) of the National Aeronautics and Space Administration (NASA; see Ricker et al. 2015) and soon the European Space Agency's (ESA's) *PLAnetary Transits and Oscillations of stars* (*PLATO*: see ESA 2017). For the same reason, that is to serve large numbers of stars, any such method should also work on spectra of moderate resolution, which are obtainable on small telescopes and cost only short exposure times.

Spectroscopic analysis is a powerful technique, eased nowadays by synthetic spectral fitting tools such as 'SOLVER' of the 'Spectroscopy Made Easy' (SME) program package (see Valenti & Piskunov 1996; Piskunov & Valenti 2017) and, more recently, the toolkit ISPEC (Blanco-Cuaresma et al. 2014, 2019), which since its 2019 version now combines several synthesis programs, including SPECTRUM (Gray 1999), TURBOSPECTRUM (Alvarez & Plez 1998), SME spectral synthesis (see above), MOOG (Sneden et al. 2012) and SYNTHE (Kurucz & Avrett 1981). Using SME and the high spectral resolving power of Keck's High Resolution Echelle Spectrometer (HIRES) spectrograph ($R = 70\,000$), Brewer et al. (2015) presented a detailed analysis of 42 *Kepler* stars, to compare purely spectroscopic and asteroseismological data. Later, Brewer et al. (2016) applied SME to 1617 planet host stars.

However, for very large stellar samples, such high-quality observational means may not be available. Fortunately, most host stars of confirmed or candidate exoplanets are bright enough to allow even a small telescope like Tracking and Imaging Gamma-Ray Experiment (TIGRE, 1.2-m aperture; see Schmitt et al. 2014) to take spectra of a more moderate, but still sufficient spectral resolution (see Section 3). In addition, with *Gaia* parallaxes, there are now additional, non-spectroscopic data of high quality available for all these stars too.

When using spectroscopic analysis on its own, parameter determination is complicated by having to fit several parameters at the same time. When one parameter is mismatched, the others are affected by cross-talk and respective systematic errors. Per se, spectroscopic analysis therefore requires a lot of attention and trying out of individual models with alternative sets of physical parameters. In particular, when it comes to work on large stellar samples, direct comparison with synthetic spectra of individual atmospheric models is simply too time-consuming.

★ E-mail: kps@astro.ugto.mx

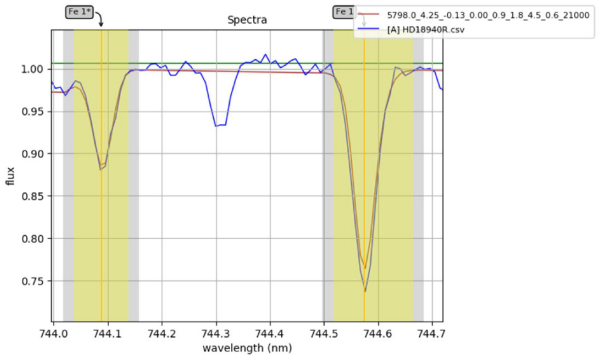

Figure 1. Showing only a very small spectral region, this figure illustrates working with the ISPEC graphic user interface (GUI).

Reducing the time-intensity of spectral fitting was the motivation for the creation of SME and, more recently, the toolkit ISPEC, a program package combining different automatized synthetic spectral analysis and fitting routines (see Blanco-Cuaresma et al. 2014, 2019 and Fig. 1 of this work). For a detailed user guide, we refer to the manual provided online with the PYTHON-based source code. This program provides automatic searches for best-match parameter sets on a library of stellar atmospheric models. In this way, ISPEC's main potential lies in a quick analysis of observed stellar spectra of high resolution, making it suitable to study large stellar samples. However, as a mere tool, ISPEC cannot escape from the ambiguities and cross-talk between different physical parameters that are created by atomic physics and radiation transport.

For this reason, we offer here a strategy to *complement any synthetic spectral fitting analysis with available, non-spectroscopic information*, in order to focus the former on the very two parameters that can be derived sensitively from spectroscopy without alternatives: effective temperature and rotation velocity. This work also advertises consistency in both the approach of synthetic spectroscopic fitting and the spectra used. Apparently, different fitting approaches on spectra of different quality, and perhaps even a lack of knowledge of the precise resolution, account for many of the differences in the physical parameters derived by different authors for the same stars.

A particularly important example is the case of rotational velocities, which are of utmost interest in the context of an angular momentum analysis of the star and how it corresponds to its present-day magnetic activity and the dynamical evolution of its planetary system. Such work requires accurate and unbiased measures of stellar rotation velocities $v \sin i$, reaching down to the slowest rotators.

However, the spectroscopic derivation of rotation velocities suffers from direct cross-talk with other quantities, when erroneous. These are, in particular, (i) the surface gravity ($\log g$) and (ii) the turbulent velocities ($v_{\rm mic}$, $v_{\rm mac}$). (iii) In addition, there are instrumental questions of direct impact. Here, we only emphasize the importance of entering a correct value for the spectroscopic resolution into the synthetic spectral fitting routine, to avoid further systematic errors of the above-mentioned physical parameters related to the line widths.

Consequently, here we are looking to resolve, or at least minimize, these problems. For this purpose, we propose a method based on the spectral analysis tool ISPEC and the complementary use of reliable external stellar information, such as parallaxes, which removes the ambiguities of a purely spectroscopic analysis by predetermining crucial parameters like gravity. This approach also offers the turbulence velocity values, well-tested here, which apply to all solar-type stars with a convective envelope, since convection is a universal phenomenon.

2 GENERAL CONSIDERATIONS OF SYNTHETIC SPECTRAL FITTING

As mentioned above, there are particular limitations that have their origin in spectroscopic physics and consequently are unavoidable in the use of any synthetic spectral fitting tool, such as ISPEC. Their nature and our resulting considerations will be explained in this work using the example of ISPEC. However, all points should apply to other means of synthetic spectral fitting as well.

ISPEC's synthesize subroutine automatically determines the physical parameters of the model atmosphere that matches the observed spectrum best, by minimizing the sum of the residuals χ^2. It can use different libraries, default choices can draw from ATLAS9 (Kurucz 1993) and MARCS (Gustafsson et al. 2008) models. Not surprisingly, it converges best with only one free parameter at a time. However, even then, a slightly lower χ^2 sum can be reached by trying different starting points around the supposed best-match value for the physical parameter in question. This problem is more prominent for the more commonly available, only moderate-resolution spectra with $R = 21\,000$, as used for this study. Blanco-Cuaresma et al. (2014) found this to be less relevant when working on very high-resolution spectra.

For the choice of the start value of effective temperature $T_{\rm eff}$, this implies using offsets of about 50–200 K. To assure the best fit of all, this means such alternative synthesize runs must be started and their χ^2 sums be compared. The reason for this complication is the often only very shallow change of χ^2 with variation of the parameter value and local minima that compete with the absolute minimum for attracting the synthesize subroutine best-match parameter solution.

Wherever there is a mismatch in one physical parameter, there is also cross-talk between it and the values found for the other quantities. Mainly, this applies to the effective temperature $T_{\rm eff}$, the surface gravity $\log g$ and the metallicity [Fe/H], which between them determine the line strengths and crucial ratios (of lines from different excitation, ionization and atomic origin). In recent work on cool giants (see Schröder et al. 2020), we had therefore set [Fe/H] and other parameters to their known values, to use only $T_{\rm eff}$ as a free parameter to be determined by the synthesize subroutine. However, when we also set the gravity $\log g$ free to be fitted as well, this quantity tended to underestimations of up to 0.5 dex, compared with its computed value. Through cross-talk, this is then compensated for (i.e. in achieving almost same lowest χ^2 sum) by a reduction of 50–100 K in $T_{\rm eff}$.

Consequently, any such underestimated surface gravity then also leads to larger-than-true rotational or turbulent velocity values, which make the line profiles compensate in the χ^2 sum. However, thanks to improving parallaxes – consider GAIA DR2 (Brown et al. 2018) and ongoing work on this cornerstone project for future use – and the ease of a reasonable mass estimate from known luminosity L and (initially an approximate value of) $T_{\rm eff}$, the gravity $\log g$ can be – and therefore should be – calculated and used as a fixed value in the synthetic spectral fitting process.

Rotational velocities are of growing interest in communities of exoplanet and stellar activity research. The cross-talk between rotation velocity and competing, physical line broadening, e.g. by turbulence and pressure damping, therefore deserves special attention. Once gravity is settled, it is mainly turbulence that is in direct competition with rotation for the observed line widths. Despite these being fundamentally different processes, resulting in different

profile shapes, they are too subtle to be distinguished directly at common spectral resolutions of, say, 20 000–50 000, especially with slow rotators – cool, aged stars like the Sun and our test stars.

As a consequence, here we define and study a sample of 25 bright stars with well-observed, long rotation periods and other physical parameters well known. In this way, these stars are particularly suitable to calibrate the turbulence velocities of solar-type stars empirically (see Section 5.2). Given the universality of convection, the result then applies to all stars of that kind.

In summary, the fast approach to spectral synthesis presented here, which we recommend for use for large stellar samples, has the following strategy (details are described further below), which aims to minimize cross-talk by maximizing the use of non-spectroscopic information and separating the assessment of quantities in direct competition for similar effects on the spectrum.

(i) Calculate approximate physical parameters from photometry and parallax, using as start values the metallicity and effective temperature of the Geneva–Copenhagen catalogue (GCC), and estimate the mass from the position in the HR diagram. Such data external to the spectroscopic analysis are available for almost all cool main-sequence stars brighter than (at least) 8 mag.

(ii) Focus spectral synthesis on one crucial parameter at a time by fixing all other parameters – in particular, gravity by its calculated value, metallicity by the GCC value, turbulence velocities by the tested values suggested below – and make sure to enter the exact value of the spectrograph resolution.

(iii) In this way, first refine the most critical parameter for spectral fitting, the effective temperature. Then revise the metallicity, with $T_{\rm eff}$ now being fixed at its best match. Repeat this step, should the metallicity now turn out to be very different from the start value.

(iv) Once the three fundamental parameters (gravity, temperature, metallicity) are all solved for and, together with the turbulence velocities, all fixed, finally free and fit the rotation velocity.

Obviously, spectral synthesis results are also affected by poor signal-to-noise ratio (S/N) and poor knowledge of the true spectrograph resolution. For these reasons, we first describe the instrumentation and spectra used for this study.

3 OBSERVATIONS AND SPECTROGRAPH PROPERTIES

The spectra of the 25 sample stars chosen for this work (see next section) were obtained with the robotic TIGRE facility in Guanajuato, central Mexico (see Schmitt et al. 2014 for a detailed description). This 1.2-m telescope is equipped with the Heidelberg Extended Range Optical Spectrograph (HEROS) echelle spectrograph, which produces spectra of good quality (typically S/N = 60–120) with a spectral resolving power $R = 21\,000$. It produces a very uniform quality over its full spectral range of 370–870 nm and, for this purpose, it is the HEROS concept to use two seperate channels and cameras (for red and blue light). In this way, the cameras and the cross-dispersers are optimized seperately in each channel. There is only a small spectral gap of 5 nm, located on the blue side of the sodium D line, which is caused by the dichroatic beam splitter.

The spectra used here have a typical effective S/N of between 70 and 80. We did not see a need to improve that by adding up a larger number of spectra, despite their availability to us. Rather, we wanted to study the precision and the limitations(!) of synthetic spectral fitting under the most common conditions. The latter include modest observational means and so justify our choice of the TIGRE–HEROS spectra. Their spectral resolving power lies well below the high end of modern high-resolution spectrographs (around $R = 120\,000$, e.g. the High Accuracy Radial velocity Planet Searcher (HARPS) spectrographs), but is more representative of what is easily available for extensive stellar studies – by use of small telescopes, which allows easier access and flexible scheduling.

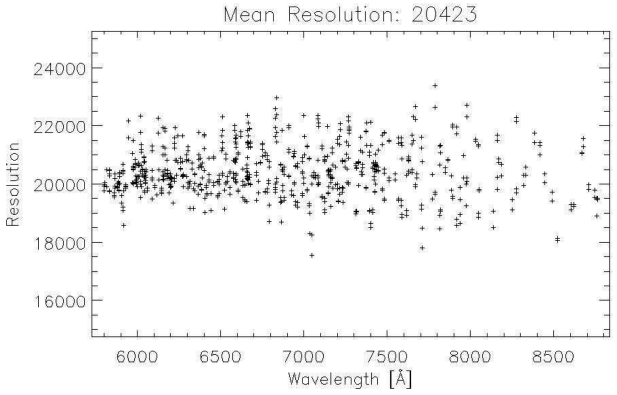

Figure 2. Resolution performance of the HEROS red channel on 2018 December 12, representative of the observing epoch of 2018/19 in the range $R \approx 19\,000$–$22\,000$; good spectra have a resolution closer to 21 000.

A trivial source of systematic error in spectroscopically derived rotation velocities is a poor specification of the true resolution of the spectrograph. For the modest spectral resolving power of HEROS, a deviation from the precise value as small as 5 per cent has a noticeable effect!

In fact, we found that, when using prescribed values for R in the range 20 000–21 000, any such 5 per cent error in R causes a systematic difference of 2–3 km s^{-1} in the outcome of rotation velocities in the fitting process. Obviously, this impact is more pronounced with modest spectral resolution, where the instrumental profile is in full competition with the true line profile and its rotational (and other) broadening factors, while it is of a lot less concern at the high end of today's spectrograph resolutions.

Hence, to start with, the spectral resolving power R must be well monitored: closely in time and to good precision. Consequently, the TIGRE–HEROS performance is monitored each night as part of the standard data reduction pipeline, which incorporates flat-fields and thorium–argon emission-line spectra taken at least twice a night.

The better spectra of TIGRE–HEROS from epoch 2018/19, in particular those used by us in this study, have in fact a spectral resolving power closer to $R = 21\,000 \pm 1000$. In this respect, Fig. 2 shows, as a representative example, the respective measurements of 2018 December 12. There is some variation within 19 000–22 000, however mostly smaller than 5 per cent of R.

Spectrum-to-spectrum or night-to-night variation of resolution may occur from the changes of seeing quality: it makes a small difference whether the seeing disc fills only 1 arcsec or the whole of the 3-arcsec large (projected on the sky) entrance lens of the optical fibre that feeds HEROS, since the normal tracking accuracy of TIGRE is better than 1 arcsec. The same effect is caused by gusty wind conditions, which briefly shake the stellar disc location on time-scales too short to compensate for by the auto-guiding of TIGRE. In addition, purely instrumental effects may also enter, such as focus issues, related to the small residual temperature and mechanical variations during each night. In the following, however, in all synthetic spectral fitting presented and discussed below, we used a fixed spectral resolution of 21 000, mainly for reasons of simplicity.

4 THE PHYSICAL PARAMETERS OF THE CALIBRATION STARS

For this work, we selected a test sample of 25 bright (4th–7th magnitude) solar-type main-sequence stars from Hempelmann et al. (2016) and (in the case of HD 140538) Mittag et al. (2019), who determined rotation periods P from high-cadence chromospheric activity monitoring with TIGRE. In this way, these stars are used by us to calibrate the turbulence velocities, while the other line-broadening factors (i.e. gravity and rotation) are known by other means.

Only stars with rotation periods longer than 10 days entered the test sample of the present work, in order to focus the work on small $v \sin i$ values, which provide the most critical test of the turbulence velocities, considering that the latter are of the order of just a few $\mathrm{km\,s^{-1}}$. In this way, this stellar test sample in the end enables calibration of the most suitable turbulence velocities, see below.

In addition, we wanted availability of the metallicity data of the Geneva–Copenhagen catalogue (Holmberg et al. 2009). These values – taken relative to the solar metallicity and thereby avoiding method-dependent differences in absolute scales – have been determined by means of *ubvy* Strømgren photometry, which, by dedicated choices of its narrow spectral bands, differentiates between Balmer lines (and their damping wings) and line-blanketing by metals, much like a spectroscopic analysis aims to do, while the effective temperature is derived from the depth of the Balmer jump.

Despite being calibrated by spectroscopic model standards of the 1980s, these *ubvy*-based metallicities are usually within a margin of 0.1 dex of the results obtained by more sophisticated, spectroscopic case studies. We therefore regard this as a good starting point for a fast synthetic spectral fitting analysis, since cross-talk with effective temperature and gravity can produce a larger error, when leaving this parameter free to be fitted as well.

For the same reason, we aim to predetermine the gravity as well, using an approximate preliminary analysis. We derive the luminosity L of these relatively near stars from their photometric data and parallaxes offered by SIMBAD (Strasbourg astronomical data centre), using the refined HIPPARCOS data of Van Leeuwen (2007). We here took this conservative choice, since the GAIA data (DR2) of bright stars and their errors still may not be sufficiently well studied. In any case, since all our calibration stars are very near, any differences are very small.

The resulting visual absolute magnitudes are therefore very trustable. To get the stellar luminosity L_* in units of the solar luminosity $\mathrm{L}_\odot$, we applied a solar visual absolute magnitude of +4.80 and a small differential bolometric correction (BC) in those cases where $B-V$ differs notably from the solar value of 0.62. This differential approach avoids any dependence on (albeit small) scale differences between different studies of BC. We based these small differential adjustments on Flower (1996, fig. 3 therein).

In the following calculation of the gravity, we used as a start value (to be refined later) for $T_{\rm eff}$ the one given by the Geneva–Copenhagen catalogue (GCC), first to find the stellar radius R of the star, employing the simple relation $L/\mathrm{L}_\odot = (R_*/\mathrm{R}_\odot)^2\,(T_{\rm eff,\,*}/T_{\rm eff,\,\odot})^4$. To estimate the mass M, we use well-tested evolution tracks to match the stellar position in the Hertzsprung–Russell (HR) diagram. In that respect, the metallicity, taken from the same catalogue (GCC), matters as well. The evolution tracks were computed by us with the evolution code version and parameterization described by Pols et al. (1997, 1998). For more details, especially on the verification of these tracks with observations and other codes, see Schröder et al. (2013, 2020) and the further references given therein.

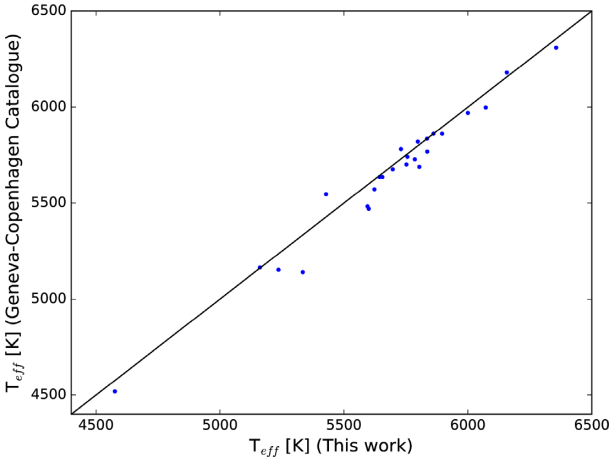

Figure 3. Comparison of Geneva–Copenhagen catalogue *ubvy* photometry based effective temperatures with those finally obtained by ISPEC for the 25 sample stars; see text and Table 1 for details. Here and in the following figure, the straight line markes a 1:1 relation.

Our results are collected in Table 1 together with the above data. Respective estimates of the uncertainties in all individual stellar parameters are as follows: (i) luminosity L: 3 per cent, resulting from under 1 per cent from parallax errors, but as much as about 2 per cent (on a relative scale) from the respective bolometric correction BC. (ii) Stellar mass M: 3–6 per cent, with a tendency of increasing uncertainty on the lower main sequence. These errors originate from the uncertainties in L and a little from the residual uncertainty of any deviation from solar metallicity. (iii) Effective temperature $T_{\rm eff}$: initial values taken from the Geneva–Copenhagen catalogue appear to be better than 2 per cent; see Table 1 comparing these values with the results of our synthetic spectral fitting. (iv) Stellar radius R: 3–5 per cent, introduced by the above uncertainties in $T_{\rm eff}$ and L. (v) Surface gravity $\log g$: 0.03–0.05 dex, according to the above errors in M and R.

Generally, we believe that these estimated errors, especially those related to gravity (0.03–0.05 dex) but also those related to metallicity (about 0.10), are a lot smaller than the typical deviations that would occur in the spectral synthesis process as a consequence of the cross-talk between a multitude of free parameters, in particular between $T_{\rm eff}$, [Fe/H] and $\log g$, amounting to perhaps as much as 0.5 dex in $\log g$. This is the reasoning behind our strategy to complement that process with calculated parameters. See Table 1 for the whole set of parameters for all 25 calibration stars used in this study.

Then, in order to test the most suitable parameters for the turbulence, we calculated, for each of the 25 calibration stars of our test sample, the respective rotation velocity $v \sin i$, using the calculated radius R and observed rotation period P. We started with the rotation velocity $v_{\rm rot} = 2\pi R/P$. Next, a realistic estimate of the average $\sin i$ value in the calibration sample is needed. We note that, for all these stars, their rotation period is evident from the variation of their activity data. It is for this reason that we may assume a minimum inclination i of *at least* 35 or 40° (i.e. $\sin i \lesssim 0.6$), taking the Sun and its active latitudes as a role model. Any active area is then still moving well out of sight, when rotated to the far side of the star. Since, on the other hand, the maximum value of $\sin i$ is 1.0, its average value in this sample is approximately 0.8, leaving us to derive the spectroscopically determined rotation to be, on average, $v \sin i \approx 0.8(\pm\,0.2) v_{\rm rot}$ (for individual values, see Table 1).

Table 1. 25 calibration stars and their physical parameters (see text for details). Compared are (i) the values for $T_{\rm eff}$ of the Geneva–Copenhagen Catalogue (GCC) with the ISPEC solutions and PASTEL means of individual spectral fitting, (ii) the rotation velocities calculated from the observed rotation periods with ISPEC's $v\sin(i)$ nominal best-fitting values (with $v_{\rm mic}$ set to values around 1 km s^{-1} and $v_{\rm mac}$ mostly to 2–3 km s^{-1}, see text for prescription details).

star	π [mas]	L_* [L$_\odot$]	[Fe/H] dex	$T_{\rm eff}^{\rm GCC}$ [K]	$T_{\rm eff}^{\rm iSp}$ [K]	$T_{\rm eff}^{\rm PSTL}(\sigma)$ [K]	R_* [R$_\odot$]	M_* [M$_\odot$]	log g [cgs]	$P_{\rm rot}$ [days]	$v_{\rm rot}^{\rm calc}(\sigma)$ [km s^{-1}]	$v\sin i^{\rm iSp}$ [km s^{-1}]
HD 18940	26.3	1.80	−0.13	5820	5798	5804(80)	1.33	1.10	4.24	10.3	6.6(2.2)	5.3
HD 19019	31.9	1.73	−0.24	5998	6072	6086(27)	1.17	1.10	4.35	13.2	4.4(1.5)	1.8
HD 20619	41.7	0.74	−0.28	5701	5752	5721(27)	0.84	0.93	4.56	21.2	2.0(0.7)	0.0
HD 22049	310.9	0.33	0.00	5152	5236	5085(70)	0.73	0.80	4.62	11.8	3.2(0.9)	0.2
HD 30495	75.5	0.92	−0.08	5781	5730	5836(41)	0.98	1.02	4.49	11.8	4.1(1.4)	0.7
HD 37394	81.4	0.45	−0.02	5140	5334	5240(80)	0.79	0.80	4.45	10.7	3.7(0.9)	0.6
HD 39881	36.4	1.45	−0.15	5689	5804	5732(21)	1.19	1.03	4.30	13.6	3.8(1.3)	0.0
HD 41330	38.8	1.90	−0.25	5861	5861	5896(30)	1.34	1.03	4.18	23.4	2.9(1.0)	0.0
HD 42807	53.6	0.80	−0.21	5636	5644	5739(19)	0.98	0.92	4.42	11.8	4.2(1.4)	1.6
HD 58855	49.0	2.30	−0.28	6310	6356	6369(61)	1.30	1.25	4.32	16.3	4.0(1.3)	9.8
HD 79028	50.9	2.62	−0.10	5861	5896	5894(62)	1.58	1.24	4.14	30.8	2.7(0.9)	5.5
HD 86728	67.0	1.31	+0.20	5741	5756	5740(59)	1.18	1.10	4.34	10.6	5.7(1.9)	3.8
HD 95128	72.5	1.52	−0.05	5835	5835	5884(52)	1.23	1.05	4.26	24.8	2.6(0.7)	1.1
HD 100623	104.8	0.39	−0.43	5164	5161	5164(67)	0.78	0.80	4.58	27.5	1.5(0.4)	0.8
HD 101501	104.4	0.63	−0.12	5483	5595	5507(82)	0.84	0.95	4.57	17.0	2.5(0.6)	0.0
HD 111395	58.5	0.90	−0.05	5546	5428	5625(25)	1.03	0.94	4.38	14.1	3.7(0.9)	1.7
HD 115617	116.9	0.95	0.00	5572	5623	5556(39)	1.02	0.95	4.40	26.5	2.0(0.7)	0.1
HD 117176	55.6	2.73	−0.12	5470	5600	5534(50)	1.84	1.10	3.95	23.4	4.0(1.4)	3.2
HD 126053	57.3	0.80	−0.39	5676	5697	5655(53)	0.93	0.90	4.45	26.3	1.8(0.6)	0.0
HD 131977	170.0	0.24	0.00	4519	4576	4607(68)	0.78	0.75	4.52	33.1	1.3(0.4)	0.0
HD 137107	60.0	1.30	−0.10	5970	6000	5994(67)	1.12	1.05	4.36	22.1	2.7(0.9)	7.0
HD 140538	67.7	0.85	−0.03	5636	5655	5679(21)	0.97	0.95	4.46	20.7	2.3(0.8)	3.4
HD 159222	41.3	1.16	+0.05	5768	5836	5794(76)	1.08	1.02	4.38	17.4	3.2(1.1)	5.0
HD 159332	25.9	6.25	−0.19	6180	6157	6197(59)	2.16	1.50	4.00	25.6	4.3(1.5)	7.5
HD 217014	64.7	1.30	+0.12	5728	5786	5773(47)	1.14	1.05	4.35	38.0	1.5(0.5)	0.7

The unknown inclination thus creates an uncertainty margin of 25 per cent. For many of our slowly rotating test stars, however, that relative error translates into a velocity error of only 0.5 km s^{-1}. In addition, there are relatively small errors in the radius of 5 per cent, but, more notably, there is an uncertainty in the period as well. Most stars (see Hempelmann et al. 2016, table A.1) were rated as sigma-class 1, meaning 1–2σ of uncertainty in their period. Hence, in relative terms, this gives an additional margin of between 10 and 30 per cent, which combines with the uncertainty of the unknown inclination. We estimate the typical total uncertainty of the calculated rotation velocity for each calibration star to be around 1 km s^{-1} or less, thanks to the selection of this sample for slow rotation – and so still good enough to test for the most suitable turbulence velocities (see next section).

5 BENCHMARK-STYLE TEST OF PROCEDURES AND TURBULENCE PARAMETERS

We were using the spectral analysis and synthetic fitting tool ISPEC, using the normalized option of the TIGRE–HEROS spectra in their red channel, as produced by our data reduction pipeline (see Schmitt et al. 2014). After loading these into ISPEC, the wavelength range was cut down to 580–875 nm, to avoid confusion from the very noisy and badly normalized ends. We then chose the Vienna catalogue of atomic line data (VALD: Piskunov et al. 1995) and loaded our list of selected lines (see Appendix A).

These lines define the segments that are the basis of the spectral synthesis process. Consequently, they were selected for their reliability in their atomic data (in fact, when the synthesize run was based on a different source of atomic data, like using the MARCS GESv5.0 list (as used by the GAIA–ESO Survey, see Gilmore et al. 2012), the resulting difference in effective temperature was only of the order of 1 K), as well as to give some variance over a range of ionization and excitation potential (which allows for sensitivity to $T_{\rm eff}$ and gravity) and to probe the chemical composition.

However, the most limiting criterion of all here is that none of these lines should suffer from blends, which would distort the χ^2 sums severely. Lines of poorly known gf values have the same effect, leading the spectral synthesis to compare with the wrong line strengths. The line list used here (see Appendix A) was developed specifically for the analysis of solar-type stars by us and was already used in earlier work (see Eisner et al. 2020). Hence, the many thousands of lines seen in the spectrum of a cool star are reduced to a number only a little over 100, which enables a sharper response of the χ^2 sums to any change in a physical parameter.

In the next work step, we determined and corrected for the radial velocity shift of the stellar spectrum relative to the laboratory wavelength scale. We then set the continuum. In the case of normalized spectra, a constant near unity suits well enough. For most HEROS spectra studied here, all of which pass our standard data reduction pipeline for calibration and normalization, we found that values in the range 1.005–1.01 gave a good continuum in the few line-free segments, i.e. leaving as much noise above as below the line. This step is critical and therefore needs to be verified closely, since any larger misfit of the continuum would cut into the upper observed line profile and so impact on the choices of the synthesize mode for parameters related to the line width, in particular the rotational velocities.

Since cool stars are crowded with many narrow lines, and for the same reasons as selecting for unblended lines in the first place, it is also advisable to use only narrow margins around each line. Consequently, we choose line segments that exceed the line width by only 0.02 nm on either side. Furthermore, we based the following parameter analysis only on the red part of the spectrum, since the blue part suffers from an even higher line density and there are hardly any lines free from blends.

The search for the best-matching physical parameters was then started using the new parameter determination by the synthesize subroutine of ISPEC (version 20190302, under pull-down menu 'Parameters', choosing 'Determine parameters and abundances with synthesis'). It finds the physical parameters by interpolating between the spectra of a library of atmospheric models, varying the free parameters and calculating the sum of the residuals χ^2 to quantify the quality of the match. In its definitions, we chose the SPECTRUM mode, which is based on the work of Gray (1999). It uses the MARCS model library and the solar abundances of Grevesse et al. (2007). However, wherever we tried alternatively with ATLAS models, the differences were marginal (in effective temperature: 1–3 K). We ran at least 15 iteration steps.

5.1 ISPEC synthesizing solutions for $T_{\rm eff}$

As explained above, we first refined the value for $T_{\rm eff}$, using this quantity as the only free (i.e. non-fixed) parameter, the others being fixed at their calculated values given by external information. The resolving power R was set to 21 000 and Grevesse, Asplund & Sauval (2007) solar abundances and the MARCS model library were chosen. At this point, the exact values of the turbulence velocities $v_{\rm mic}$ and $v_{\rm mac}$ did not yet play a role.

Any $T_{\rm eff}$ value found by ISPEC in its first run was then used as a new start point to see whether it would be reproduced again. In addition, alternative starting points 50–200 K away were used, in an attempt to find an even smaller sum of residuals χ^2 of an even better match further away from the first solution.

When this stage was reached, we applied a further test: to fix the value found for $T_{\rm eff}$ and free either metallicity or gravity. ISPEC then either maintained exactly those values as a best fit or suggested close alternatives, within 0.05 dex. For this, the velocity values for the turbulence and rotation parameters had to be already near their final values; see below. These test results we consider as reassurance regarding our method to predetermine gravity and metallicity.

Table 1 lists the values of $T_{\rm eff}$ finally obtained for each star by ISPEC and compares them with the respective values in the Geneva–Copenhagen catalogue, which we used as a start value for the run of the synthesize subroutine. See also Fig. 3 for a comparison of these two sets.

The differences between the final synthetic spectral fitting result for the effective temperature in ISPEC and the value given by the Geneva–Copenhagen catalogue show a variance of 63 K and so coincide mostly within 1 per cent. There is a small offset of 38 K between these two sets, which should not surprise us, considering that the *ubvy*-photometry based assessment was calibrated with the standards and atmospheric models of the 1980s. Rather, we are surprised by how good the coincidence is. This certainly justifies the idea to use the Geneva–Copenhagen catalogue for start values to accelerate the synthetic spectral fitting analysis.

To compare our effective temperatures, obtained so economically with ISPEC, with those found by much more time-consuming studies (many of these are individually matching model atmospheres to the observed spectra, including in some cases the use of spectra with much higher resolution), in Fig. 4 we compare our quick $T_{\rm eff}$ results with the medians of the entries in the PASTEL catalogue (Soubiran et al. 2016, version 2020-01-30 in VizieR) – i.e. we simply averaged on a logarithmic scale. Only HD 18940 has only one entry. The variance of the $T_{\rm eff}$ values is similarly small (71 K) to that above. While it cannot be said on which side of the comparison these differences arise, we note that at least the systematic offset has effectively (nominally 4 K) disappeared. This should be expected, because ISPEC draws from the same generation of newer atmospheric models as individual spectroscopic studies of the past decade. However, any wrong-leaning of other values (gravity and metallicity, in particular) could, via cross-talk, still shift the distribution of effective temperatures found by synthetic spectral fitting – at least this does not happen with our approach in any systematic way.

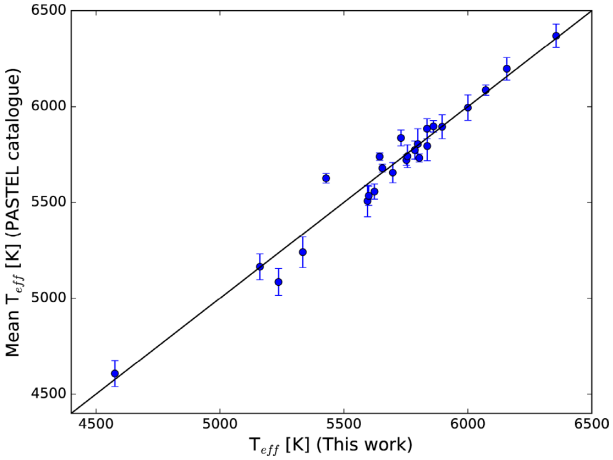

Figure 4. Comparison of PASTEL catalogue means of effective temperature with those finally obtained by ISPEC in this work for the 25 sample stars.

5.2 Prescribing turbulence for synthesis of $v\sin i$

Once the main stellar physical parameters are settled in the manner described here, the relative and absolute line strengths (equivalent widths) of the best-matching synthetic spectrum match those of the selected lines of the observed stellar spectrum best. This now leaves the final adjustment required to use the line widths. Given that gravity is a known quantity and fixed, here only turbulence and rotation velocities compete for the line width. Using the above 25 calibration stars of known rotation velocities, turbulence parameters can be calibrated to deliver the known rotation velocities in the synthesizing mode of ISPEC (or any other comparable tool).

Since convection is a universal process, those turbulence velocities should apply equally to all stars with the same physical parameters. ISPEC is therefore using a prescription to give a choice by default, which for most of our test stars suggests values of 1 km s^{-1} for the effects of microturbulence and 4 km s^{-1} for macroturbulence. In earlier work on moderate- to fast-rotating stars, these values seemed to be good enough. However, coming to aged stars and their slow rotation now brings any velocity assessment to its most critical test. Consequently, here we use our sample of 25 well-observed slowly rotating stars to improve the choice of turbulent velocities for use with the ISPEC synthesize fitting of rotational velocities. While, with the modest spectral resolving power of $R = 21\,000$ exercised here, rotation velocities under 3 km s^{-1} cannot be specified, such slow rotators are a good test for the choice of prescription of the turbulence parameters.

Ryabchikova et al. (2016) recently presented a detailed empirical study of the turbulent velocities of cool main-sequence stars using very high resolution and S/N HIRES spectra from Keck and analysis with SME – see, in particular, their fig. 7. With the lower resolution of TIGRE–HEROS spectra in mind, we simplify their results to form a prescription, as follows. The microturbulence rises slowly from 0.7 km s^{-1} around 5000 K (and under) to 1.0 km s^{-1} around 5700 K, the temperature range of most of our sample stars, and then a little faster to about 1.5 km s^{-1} at 6300 K (the warm limit of stars). In the same temperature range, the empirical macroturbulence values of Ryabchikova et al. (2016) rise from about 2.5 to 3 km s^{-1} (5000 to 5700 K), then steepen to reach 6 km s^{-1} for only our warmest stars around 6300 K. We have chosen these empirical findings for use in our study. While they are not very different from the ISPEC own prescription, the empirical macroturbulence is a little lower among the cooler sample stars.

With this prescription of the turbulence velocities, the small (calculated) rotation velocities of our slow-rotating sample stars are indeed matched well enough by the $v \sin i$ values that are then produced by ISPEC synthesis (see Table 1 for the complete list). The average residual of the latter against the calculated rotation velocity is 2.5 km s^{-1}. This variance is consistent with the above-mentioned limitations due to the modest spectral resolution.

Convection is a universal phenomenon, and therefore we expect these results to apply to all other stars of the same kind, by their fundamental physical parameters, as our sample stars. Therefore, the simple approach described here applies to cool main-sequence stars in general.

By common sense, it can be assumed that a significantly higher spectral resolving power (as with spectra obtained by ESO-UVES, HIRES, SONG, HARPS) leads to a better consistency of the fitting process, at best 1 km s^{-1} (see e.g. Fuhrmann 2004). Consequently, with such better observational material, it is even more important to use the best synthesizing approach and to fix certain parameters most accurately, i.e. according to the work of Ryabchikova et al. (2016), so as to minimize any cross-talk. However, as pointed out before, for practical aspects (economizing of observing resources to reach large samples), this article is deliberately focusing on moderate resolution spectra, which are easier to obtain for large stellar samples, and simplicity of the approach.

A minor systematic effect seems to remain: the three stars with the largest $v \sin i$ are also the three warmest stars of the sample, so that residual, temperature-dependent cross-talk could be suspected.

In this respect, a possible culprit is the single sample of reference lines that we used for the synthesize process on all stars, regardless of their effective temperature. This line sample may still require complementing for more lines typical of warmer stars. Obviously, further work on creating and testing better sets of lines for stars that are significantly warmer or cooler than the Sun will still improve the precision of parameters derived with ISPEC or equivalent spectral synthesizing tools. Nevertheless, we find that ISPEC's synthesize subroutine yields a high accuracy, considering the moderate spectral resolution used here to test it and despite a very time-economic approach with this tool.

6 CONCLUSIONS

We have highlighted the problems of spectroscopic analysis in general and of stellar parameter assessment by synthetic spectral fitting in particular. In the presence of different studies – which all use different spectroscopic methods, different atmospheric models and different synthetic spectral fitting tools and strategies, as well as spectra of different quality and resolution – we hope we have raised some awareness of how inconsistent such results consequently are and that there is the need for a consistent and well-tested approach to the assessment of stellar parameters in a larger sample.

We here have shown the potential of fast spectral synthesis, applied to only modest spectral resolution, when these are in fact combined with complementary non-spectroscopic data, such as parallaxes, to predetermine some physical parameters (like gravity), which are otherwise not determined well by spectroscopic analysis alone.

This work leads to two conclusions. First, and this despite all complications in any spectroscopic analysis, which originate in the processes of line formation, we have shown that ISPEC and other, comparable synthetic spectral fitting tools allow us to obtain accurate effective temperatures in a very short time – as long as a strategy is used in which complementary, non-spectroscopic information supports the synthetic spectral fitting process. In particular, the approach proposed here strongly reduces the number of parameters to be determined by the latter. The fast and nevertheless precise working of ISPEC in this context is certainly good news for upcoming studies of larger stellar samples in the research areas of exoplanet physics and stellar activity.

Secondly, having used 25 well-known stars for calibrating the turbulence velocities to be entered into the synthetic fitting process, we find that a prescription based on the empirical values found by Ryabchikova et al. (2016) is the most reliable one. In fact, with values of mostly around 1 km s^{-1} for the microturbulence and around 2–3 km s^{-1} for the macroturbulence of most of our cool main-sequence stars (but rising to over 6 km s^{-1} for effective temperatures above 6300 K), the rotation velocities fitted by ISPEC are reliable within about 3 km s^{-1} (with residuals of 2.5 km s^{-1} against period-related rotation velocities) for spectra with a modest resolving power $R = 21\,000$.

However, we should end with a note of caution. Uncertainties of a systematic nature, arising from the necessary simplifications in every atmospheric modelling code, as well as from the use of 1D convection models, of course remain untested in this study.

Nevertheless, with this work we see the way now paved for studies that will yield more accurate and consistent relations of stellar rotation with magnetic activity and exoplanet properties, to name only the most obvious application. Since very large stellar samples are now to be studied in such a context, it is important that such undertakings are swift and that moderate-resolution spectra will be sufficient – as long as their quality is very well known. We demonstrated here that all this is indeed possible, without sacrificing accuracy, when information external to spectral synthesis is used in a strategic and consistent way to avoid cross-talk between parameters.

ACKNOWLEDGEMENTS

Above all, the authors acknowledge the great work done by Sergi Blanco-Cuaresma, CfA Harvard, to create the easy-to-use tool ISPEC, which facilitates spectral analysis and parameter synthesis enormously. Furthermore, we are grateful for travel support by the bilateral Conacyt-DFG grant No. 278156, which supported the research visits and conference participation of four authors (KPS, MM, LMFT, DJ). Finally, we thank our referee, Tatiana Ryabchikova, for very valuable suggestions, which have improved this publication.

DATA AVAILABILITY

The data underlying this article are available in the article.

REFERENCES

Alvarez R., Plez B., 1998, A&A, 330, 1109
Blanco-Cuaresma S., 2019, MNRAS, 486, 2075
Blanco-Cuaresma S., Soubiran C., Heiter U., Jofré P., 2014, A&A, 569, A111
Brewer J. M., Fisher D. A., Basu S., Valenti J. A, Piskunov N., 2015, ApJ, 805, 126B
Brewer J. M., Fisher D. A., Basu S., Valenti J.A, Piskunov N., 2016, ApJS, 225, 32
Brown A. G. A.(GAIA collaboration) et al. (GAIA collaboration), 2018, A&A, 616, A1
Eisner N. L. et al., 2020, MNRAS, 494, 750
ESA, 2017, PLATO Definition Study Report, ESA-SCI(2017)1, European Space Agency, Noordwijk, NL
Flower P. J., 1996, ApJ, 469, 355
Fuhrmann K., 2004, Astron. Nachr.,325, 1
Gilmore G. et al., 2012, ESO Messenger, 147, 25
Gray R. O., 1999, ASCL, 9910.002
Grevesse N., Asplund M., Sauval A. J., 2007, Space Sci. Rev.,130, 105
Gustafsson B., Edvardsson B, Eriksson K., Jøgensen U. G., Nordlund Å., Plez B., 2008, A&A, 592, A70
Hempelmann A., Mittag M., González-Pérez J. N., Schmitt J. H. M. M., Schröder K. P., Rauw G., 2016, A&A, 586, A14
Holmberg J., Nordstrom B., Andersen J., 2009, A&A, 501, 941
Kurucz R., 1993, ATLAS9 Stellar Atmosphere Programs and 2 km/s grid, Smithsonian Astrophysical Observatory, Cambridge, MA
Kurucz R., Avrett E. H., 1981, SAO Spec. Rep., 391, 1
Mittag M., Schmitt J. H. M. M., Metcalfe T. S., Hempelmann A., Schröder K. P., 2019, A&A, 628, A107
Piskunov N., Valenti J. A., 2017, A&A, 597, A16
Piskunov N. E., Kupka F., Ryabchikova T. A., Weiss W. W., Jeffery C. S., 1995, A&AS, 112, 525
Pols O. R., Tout C. A., Schröder K.-P., Eggleton P. P., Manners J., 1997, MNRAS, 289, 869
Pols O. R., Schröder K.-P., Hurley J. R., Tout C. A., Eggleton P. P., 1998, MNRAS, 298, 525
Ricker G. R., et al., 2015, J. Astron. Telescopes, Instruments, and Systems, 1, 1
Ryabchikova T. et al., 2016, MNRAS, 456, 1221
Schmitt J. H. M. M. et al., 2014, Astron. Nachr., 335, 787
Schröder K.-P., Pols O. R., Eggleton P. P., 1997, MNRAS, 285, 696
Schröder K.-P., Mittag M., Hempelmann A., González-Pérez J. N., Schmitt J. H. M. M., 2013, A&A, 554, A50
Schröder K.-P., Mittag M., Jack D., Rodríguez Jiménez A., Schmitt J. H. M. M., 2020, MNRAS, 492, 1110
Sneden C., Bean J., Ivans I., Lucatello S., Sobeck J., 2012, ASCL, 1202.009
Soubiran C., Le Campion J.-F., Brouiliet N., Chemin L., 2016, A&A, 591, A118
Valenti J. A., Piskunov N., 1996, A&AS, 118, 595
Van Leeuwen F., 2007, A&A, 474, 653

APPENDIX A

Table A1 contains the list of selected lines used by us with iSPEC to determine the physical parameters in the synthesize mode. For solar-type stars, these lines are relatively free of blends and have reliable atomic data.

Table A1. List of lines selected for use with the iSPEC synthesize subroutine.

λ_0/nm	λ_{blue}/nm	λ_{red}/nm	Note
588.99222	588.94222	589.04222	Na 1∗
589.59111	589.54111	589.64111	Na 1∗
593.01786	592.98592	593.05392	Fe 1∗
593.46382	593.42892	593.50592	Fe 1
595.67061	595.62061	595.72061	Fe 1∗
597.53979	597.48979	597.58979	Fe 1∗
597.67737	597.62991	597.72291	Fe 1∗
598.48094	598.43190	598.56890	Fe 1∗
598.70582	598.64490	598.75990	Fe 1∗
600.29994	600.25190	600.35090	Fe 1
600.85379	600.82490	600.89890	Fe 1
601.66100	601.61100	601.71100	Fe 1
602.01367	601.96367	602.06367	Fe 1
602.40547	602.35789	602.46389	Fe 1
605.59974	605.55988	605.68088	Fe 1
606.54840	606.50088	606.59188	Fe 1
607.84832	607.77287	607.87687	Fe 1
608.26795	608.21795	608.31795	Fe 1
608.52749	608.47749	608.57749	Fe 1
612.22026	612.17026	612.27026	Ca 1
615.16083	615.11083	615.21083	Fe 1
616.21895	616.16895	616.26895	Ca 1
617.04985	617.00284	617.11684	Fe 1
617.33263	617.28284	617.38384	Fe 1
621.34219	621.29882	621.39582	Fe 1
621.92807	621.84182	621.96982	Fe 1
623.07270	623.02782	623.18682	Fe 1
623.26354	623.18682	623.30782	Fe 1
624.63196	624.58981	624.68681	Fe 1
625.25592	625.21081	625.31081	Fe 1
625.42234	625.32981	625.50981	Fe 1
625.63286	625.56281	625.67981	Fe 1
629.09733	629.04733	629.14733	Fe 1
629.77983	629.71379	629.85479	Fe 1
630.14957	630.08979	630.20279	Fe 1∗
630.24907	630.20279	630.30279	Fe 1∗
632.26928	632.22279	632.31279	Fe 1
633.53182	633.46578	633.58878	Fe 1
633.68303	633.63878	633.74778	Fe 1
635.50570	635.44677	635.57677	Fe 1
635.86823	635.81277	635.92577	Fe 1
638.07640	638.02640	638.12640	Fe 1
639.36090	639.29676	639.42776	Fe 1
640.80071	640.75776	640.91376	Fe 1
641.16448	641.08775	641.21975	Fe 1
641.69490	641.64490	641.74490	Fe 2
641.99210	641.94275	642.04075	Fe 1
642.13587	642.07575	642.20975	Fe 1
643.08403	643.01575	643.15275	Fe 1
643.26813	643.21813	643.31813	Fe 2∗
643.90724	643.85724	643.95724	Ca 1
645.63656	645.58656	645.68656	Fe 2
646.25808	646.20808	646.30808	Ca 1
646.92107	646.87107	646.97107	Fe 1∗
647.56171	647.51171	647.61171	Fe 1∗
648.18618	648.13618	648.23618	Fe 1∗
649.49799	649.41973	649.54373	Fe 1
651.60867	651.55867	651.65867	Fe 2∗
651.83680	651.78680	651.88680	Fe 1∗
654.62497	654.57571	654.69671	Fe 1
656.27883	655.54830	656.68319	H 1∗
656.91794	656.85270	656.97870	Fe 1
657.50074	657.45074	657.55074	Fe 1∗
659.38784	659.34169	659.45369	Fe 1∗
659.75725	659.70725	659.80725	Fe 1
660.91047	660.86047	660.96047	Fe 1
664.36386	664.31386	664.41386	Ni 1
667.79785	667.72966	667.87066	Fe 1
670.50702	670.45702	670.55702	Fe 1

Table A1 – *continued*

Table A1 – *continued*

λ_0/nm	λ_{blue}/nm	λ_{red}/nm	Note
671.30728	671.25728	671.35728	Fe 1
671.76380	671.71380	671.81380	Ca 1
672.66776	672.61776	672.71776	Fe 1
675.01525	674.96525	675.06525	Fe 1
680.68577	680.63577	680.73577	Fe 1
682.03944	681.98944	682.08944	Fe 1
682.85851	682.80851	682.90851	Fe 1
683.98106	683.93106	684.03106	Fe 1
684.36502	684.31502	684.41502	Fe 1
691.67181	691.62181	691.72181	Fe 1∗
693.36353	693.31353	693.41353	Fe 1∗
694.52032	694.47032	694.57032	Fe 1
695.12212	695.07212	695.17212	Fe 1∗
703.82181	703.77181	703.87181	Fe 1
706.84183	706.79183	706.89183	Fe 1∗
709.03504	708.98504	709.08504	Fe 1
713.09510	713.04510	713.14510	Fe 1∗
713.29527	713.24527	713.34527	Fe 1
714.52678	714.47678	714.57678	Fe 1
714.81661	714.76661	714.86661	Ca 1
715.56246	715.51246	715.61246	Fe 1∗
716.44734	716.31849	716.50849	Fe 1∗
717.59031	717.54031	717.64031	Fe 1∗
721.96340	721.91340	722.01340	Fe 1
722.11903	722.06903	722.16903	Fe 1
724.48117	724.43117	724.53117	Fe 1∗
732.06783	732.01783	732.11783	Fe 1∗
738.63181	738.58181	738.68181	Fe 1

Table A1 – *continued*

λ_0/nm	λ_{blue}/nm	λ_{red}/nm	Note
738.93798	738.84541	738.99741	Fe 1
741.11487	741.03940	741.17640	Fe 1
742.22695	742.17695	742.27695	Ni 1
744.08772	744.03772	744.13772	Fe 1∗
744.57448	744.51739	744.66539	Fe 1
749.50489	749.44838	749.57237	Fe 1
751.10223	751.00237	751.18537	Fe 1
771.03274	770.98274	771.08274	Fe 1∗
772.32244	772.27244	772.37244	Fe 1
774.82964	774.76529	774.86129	Fe 1
775.11252	775.06252	775.16252	Fe 1
778.05543	777.96128	778.12627	Fe 1
783.21983	783.14526	783.31826	Fe 1
793.71440	793.61122	793.78022	Fe 1
794.58381	794.51322	794.65022	Fe 1
799.89586	799.81120	799.96220	Fe 1
804.60522	804.52818	804.70018	Fe 1
808.51700	808.44417	808.60117	Fe 1∗
820.77842	820.72842	820.82842	Fe 1
832.70659	832.63408	832.77108	Fe 1∗
838.77489	838.70606	838.85206	Fe 1∗
846.84327	846.78203	846.89303	Fe 1
851.40418	851.32902	851.46502	Fe 1
868.85943	868.77596	868.94296	Fe 1
871.03947	870.98947	871.08947	Fe 1

This paper has been typeset from a TEX/LATEX file prepared by the author.